Journal of Molecular Structure: THEOCHEM 942 (2010) 66–70

Contents lists available at ScienceDirect

Journal of Molecular Structure: THEOCHEM

journal homepage: www.elsevier.com/locate/theochem

Theoretical study on the reaction of Be(^{3}P) with methane

Yuanqin Yu [a,*], Feng Yu [b], Xiaoguo Zhou [b]

[a] School of Physics and Material Science, Anhui University, Hefei, Anhui 230039, China
[b] Hefei National Laboratory for Physical Sciences at the Microscale, Department of Chemical Physics, University of Science and Technology of China, Hefei, Anhui 230026, China

ARTICLE INFO

Article history:
Received 23 September 2009
Received in revised form 15 November 2009
Accepted 24 November 2009
Available online 3 December 2009

Keywords:
Reaction mechanism
Be atom
Methane
Steric hindrance

ABSTRACT

The reaction mechanism of Be(^{3}P) with CH_4 has been investigated theoretically at the QCISD(T)/6-311++G(d,p)//UB3LYP/6-311G(d) levels. It is shown that the excited Be atom can readily insert into C–H bond of methane without a barrier and the reaction proceeds through the insertion intermediate H–Be–CH_3(^{3}A′) followed by three processes, i.e., direct decomposition, rearrangement and intersystem crossing. Five possible reaction channels, yielding organoberyllium compounds BeH, $BeCH_3$, $HBeCH_2$, HBeCH and $HBeCH_3$(^{1}A_1), respectively, have been examined. The high reactivity of Be(^{3}P) atom with methane is supposed to be due to small steric hindrance compared with other group 2 and 12 metal atoms. Our results well rationalize the experimental observations.

1. Introduction

The C–H bond activation of methane by bare metal atoms has attracted much attention in the past three decades, due to its application in the petrochemistry and organometallic chemistry as well as conversion of nature gas to other valuable products such as ethylene. A large number of experimental and theoretical studies have been carried out to elucidate the mechanism of reaction M + CH_4, where M is a metal atom, such as Zn, Cd, Hg [1–10]. No apparent interaction was observed between CH_4 and ground-state atoms, whereas photo excited metal atoms were shown to insert into C–H bond with the formation of corresponding intermediates H–M–CH_3.

To compare the capability of different metal atoms to activate C–H bond, Greene et al. has systematically examined the reaction of CH_4 with a serials of excited state metal atoms by low-temperature matrix IR spectra technique, including group 2 metal atoms Be, Mg, Ca [11], group 12 Zn, Cd, Hg [12] and group 13 Ga, In [13]. Among these atoms, they found that the Be atom exhibited especially high reactivity with methane and produced abundant organoberyllium compounds compared with other metal atoms. The reaction pathways include

$$\begin{aligned} Be(^3P) + CH_4 &\rightarrow CH_3 + HBe \\ &\rightarrow H + BeCH_3 \\ &\rightarrow H + HBeCH_2 \\ &\rightarrow H_2 + HBeCH \\ &\rightarrow HBeCH_3(^1A_1) \end{aligned}$$

Obviously Be(^{3}P) is an effective methane activation reagent and the reaction also provides a good way to synthesize organoberyllium hydrides, HBeR, which are subject to oligomerization and polymerization processes [12]. Although they predicted the reaction proceeded via an insertion-elimination mechanism, the explicit information on the structures and energies of all intermediates and transition states involved in the reaction still remained unclear. On the other hand, we know that Be atom has similar valance structure with other group 2/12 metal atoms Mg, Zn, Cd and Hg. Why it is more efficient in reaction with methane? Recent experimental and theoretical studies revealed that many transition metals such as Re and Pt were good C–H insertion agents in reactions with small alkanes and the high reactivity of these transition metal atoms was mainly influenced by d-orbital electrons [14–17]. Since Be(^{3}P) atom has only two valance electrons 2s and 2p what may determine its high reactivity with methane. To better understand the reaction mechanism, we present here a theoretical study on the reaction of Be(^{3}P) + CH_4. The calculated results are expected to explain the experimental observations.

2. Computational methods

The DFT-B3LYP method was applied to study the title reaction [18,19]. The optimized geometries, harmonic vibrational

* Corresponding author. Tel.: +86 551 5108049; fax: +86 551 5107237.
E-mail address: yyq@ahu.edu.cn (Y. Yu).

0166-1280/$ - see front matter © 2010 Published by Elsevier B.V.
doi:10.1016/j.theochem.2009.11.037

frequencies and zero point energies (ZPE) of all stationary points (reactants, products, intermediates and transition states) were calculated at the UB3LYP/6-311G(d) level. The intrinsic reaction coordinate (IRC) calculations were used to track minimum energy paths from transition states to the corresponding reactants and products. To obtain more accurate relative energies, the single-point energies were calculated at the QCISD(T)/6-311++G(d,p) level with UB3LYP/6-311G(d) optimized geometries and ZPE. All calculations were carried out using the GAUSSIAN03 program package [20].

3. Results and discussion

To fully understand the reaction mechanism of Be(^{3}P) with CH_4, the reaction pathways are both investigated on the triplet excited state (2s2p, ^{3}P) and the singlet ground-state (2s2s, ^{1}S) of Be. The optimized structures of various species in the reaction are described in Fig. 1, including the reactants, intermediates, transition states and products. The relative energies of all species calculated at the UB3LYP/6-311G(d) and QCISD(T)/6-311++G(d,p) levels are listed in Table 1. The potential energy diagrams along the reaction

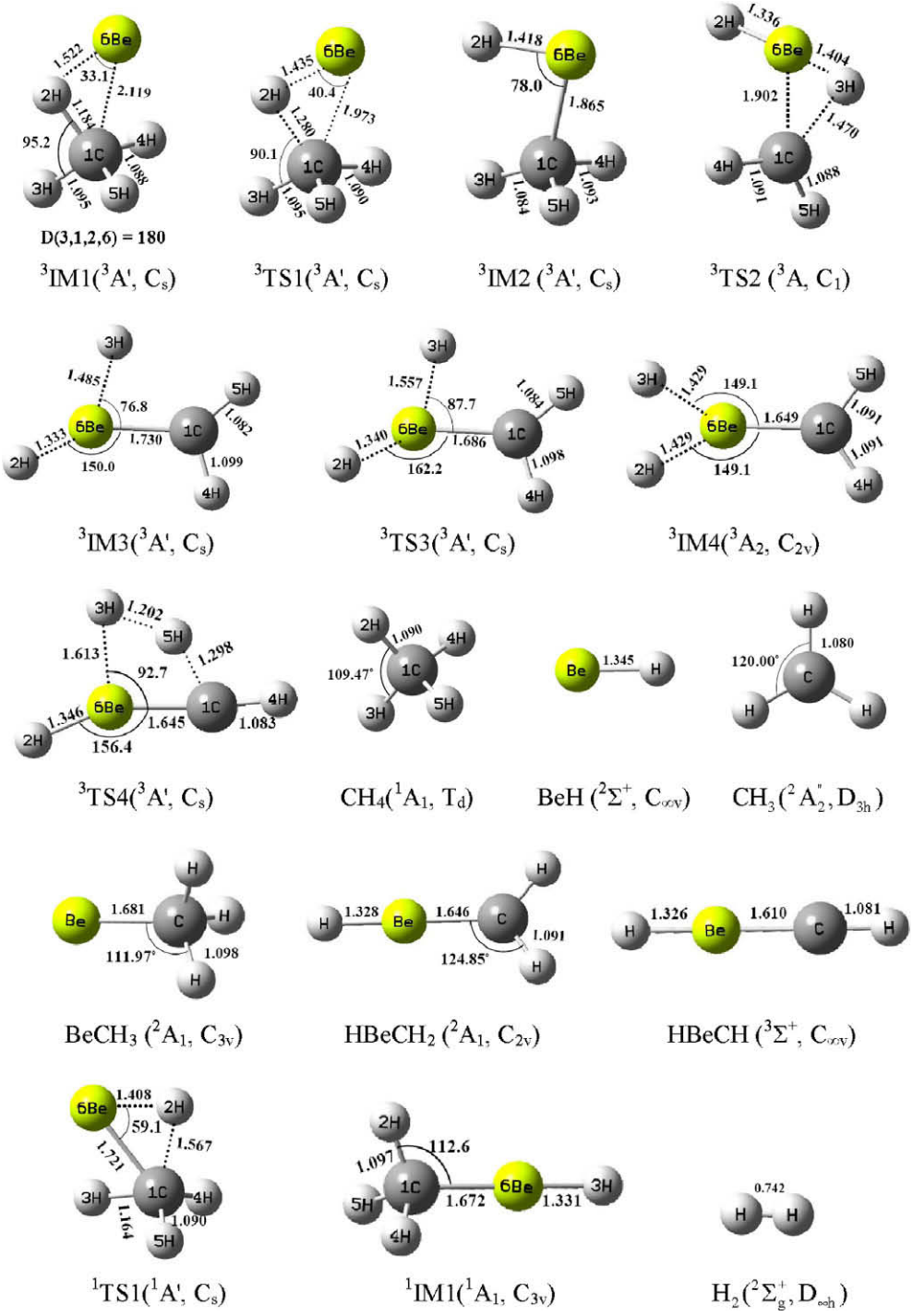

Fig. 1. Optimized geometries (distance in Å and angle in degree) for the stationary points on both triplet surface of Be(^{3}P) + CH_4 and singlet surface of Be(^{1}S) + CH_4 at the UB3LYP/6-311G(d) level.

Table 1
The ZPE (Hartree), total energies (E_T, Hartree), relative energies (E_R, kcal/mol) corrected by ZPE, and imaginary frequency for transition states.

Species	UB3LYP/6-311G(d)				QCISD(T)/6-311++G(d,p)	
	ZPE	E_T	E_R	Imaginary	E_T	E_R
$Be(^3P) + CH_4$	0.0430	−55.1086	0.0		−54.9222	0.0
$^3IM1$	0.0420	−55.1131	−3.5		−54.9260	−3.0
$^3TS1$	0.0395	−55.1129	−5.0	420i	−54.9245	−3.6
$^3IM2$	0.0379	−55.1255	−13.8		−54.9317	−9.1
$^3TS2$	0.0319	−55.0922	3.4	1124i	−54.8984	8.0
$^3IM3$	0.0329	−55.1091	−6.7		−54.9121	0.0
$^3TS3$	0.0312	−55.1084	−7.3	392i	−54.9099	0.3
$^3IM4$	0.0331	−55.1219	−14.5		−54.9223	−6.3
$^3TS4$	0.0274	−55.0727	12.8	1122i	−54.8759	19.2
$CH_3 + HBe$	0.0328	−55.1128	−9.0		−54.9244	−7.8
$H + BeCH_3$	0.0335	−55.1114	−7.7		−54.9234	−6.7
$H + HBeCH_2$	0.0287	−55.1032	−5.5		−54.9114	−2.2
$H_2 + HBeCH$	0.0280	−55.1149	−13.3		−54.9250	−11.1
$Be(^1S) + CH_4$	0.0430	−55.1990	−56.7		−55.0235	−63.5
$^1TS1$	0.0371	−55.1076	−3.1	1417i	−54.9210	−3.0
$^1IM1$	0.0410	−55.2653	−99.6		−55.0720	−95.2

coordinate on the triplet and singlet surfaces are shown in Figs. 2 and 3, respectively. The crossing points between two surfaces are located by means of the intrinsic reaction coordinate (IRC) approach and shown in Fig. 4. The calculated vibrational frequencies (scaled by 0.96) and corresponding IR intensities are listed in the Table S1 of Supplementary material and the results indicate that the calculated frequencies for the products are in good agreement with experimental ones. The reaction mechanism will be discussed on the triplet and singlet surfaces as follows, respectively.

3.1. Triplet potential energy surface

3.1.1. Insertion

Previous theoretical investigations on the reaction of metal atom with CH_4 suggest that the insertion of metal atom is a key step to activate C–H bond. In the present reaction of $Be(^3P) + CH_4$, the excited Be atom firstly approaches CH_4 along the gap between 2H and 4H atoms and then side-on attacks one C–H bond to form a precursor complex, $^3IM1$, which is bound by 3.0 kcal/mol relative to the reactants and has Cs symmetry, as shown in Figs. 1 and 2. As a result, the C–2H bond is elongated to 1.184 Å as compared to the corresponding C–H bond (1.090 Å) in free CH_4. According to vibrational mode analysis, the frequency of 1802 cm^{-1}, which is assigned as the C–2H stretching mode of CH_4 moiety, is smaller than that of free CH_4 (3019 cm^{-1}). These results indicate that C–2H bond of CH_4 moiety has been partially activated by $Be(^3P)$ atom at the initial step of the reaction.

Following $^3IM1$, the Be atom will insert into C–H bond to form intermediate H–Be–CH_3($^3IM2$) via the three-member ring transition state $^3TS1$, which lies 3.6 kcal/mol below the initial reactants. As can be seen from Fig. 1, the geometries of $^3TS1$ and $^3IM2$ are similar and the main differences consist in that C–2H bond is further elongated to be thoroughly broken while C–Be and Be–2H bonds are shortened, from 1.973 Å and 1.435 Å to 1.865 Å and 1.418 Å, respectively. In addition to the changes of bond lengths, there are also significant changes in the insertion angle C–Be–2H and it takes the value of 40.4° and 78.0° in $^3TS1$ and $^3IM2$, respectively. In Fig. 2, one may note that $^3IM1$ is slightly higher than $^3TS1$ with 0.6 kcal/mol. From the Table 1, it can be seen that the total energy of $^3IM1$ is very close to that of $^3TS1$ and ZPE-correction places $^3IM1$ slightly above $^3TS1$. If the ZPE-correction is not included, $^3IM1$ would be lower than $^3TS1$. Although the energetic order between $^3IM1$ and $^3TS1$ is reverse,

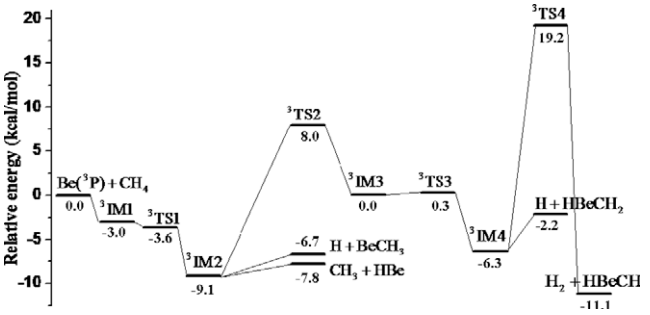

Fig. 2. The potential energy diagram of the reaction $Be(^3P) + CH_4$ calculated at the QCISD(T)/6-311++G(d,p)//UB3LYP/6-311G(d) levels.

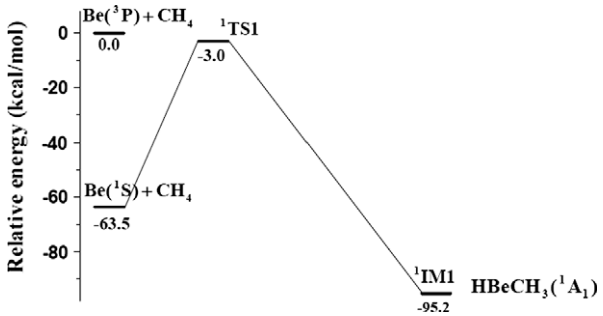

Fig. 3. The potential energy diagram of the reaction $Be(^1S) + CH_4$ calculated at the QCISD(T)/6-311++G(d,p)//UB3LYP/6-311G(d) levels.

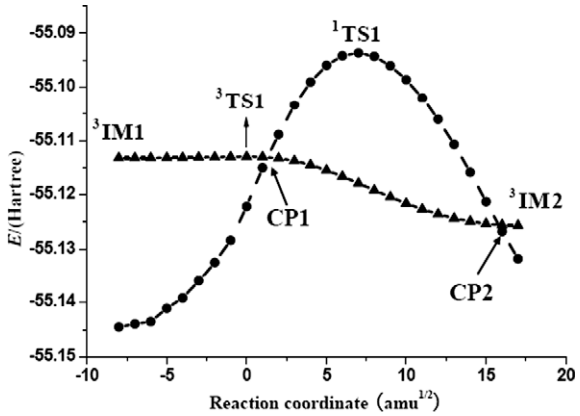

Fig. 4. IRC profile from $^3IM1$ to $^3IM2$ for the triplet surface and corresponding single-point energies for the singlet surface calculated at UB3LYP/6-311G(d) level. Two crossing points are located and labeled as CP1 and CP2, respectively.

^{3}TS1 can be verified to be a true transition state at higher levels of QCISD/6-311G(d) and CCSD/6-311G(d), as listed in the Table S2 of Supplementary material. And IRC calculations demonstrate that ^{3}TS1 truly connects ^{3}IM1 and ^{3}IM2.

As indicated in PES of Fig. 2, the process of insertion of Be(^{3}P) into C–H bond is spontaneous with no activation barrier. This agrees with the observed high reactivity of Be(^{3}P) with CH_4 compared with other group 2/12 metal atoms Mg, Zn, Cd and Hg, which have similar valance structures to Be(^{3}P). The next question is why the Be atom is more efficient in reaction with methane. The previous studies revealed that the high reactivity of some transition metal atoms such as Re and Pt was mainly influenced by the d-orbital electrons, including the number of d electrons and the energy of the d-block orbital [14–17]. Since Be(^{3}P) atom has no d electrons the high reactivity of Be with CH_4 should be from other factors.

Several groups have comparatively investigated the reactions M(^{3}P) + CH_4 and M(^{3}P) + SiH_4, where M = Zn, Cd, Hg, and found that these atoms could spontaneously insert into Si–H bond of SiH_4 but they must pass over a certain barrier to insert into C–H bond of CH_4 [4–6,21–24]. For Zn, Cd and Hg, the activation barriers were 18, 27 and 13 kcal/mol, respectively. The differences in reactivity of Zn, Cd, Hg with CH_4 and SiH_4 were ascribed to steric hindrance, which resulted in easier insertion for SiH_4, since the Si–H bond (1.5 Å) in SiH_4 was longer than the C–H bond (1.1 Å) in CH_4. It is well known that Be is the lightest metal atom except for Li and its bulk is very small. Therefore, according to the above viewpoint, the high reactivity of Be(^{3}P) with CH_4 can also be supposed to be due to small steric hindrance. This can also be confirmed in the recent theoretical investigation on the reactions of BeO + CH_4 [25] and ZnO + CH_4 [26], where the calculations demonstrated that BeO + CH_4 proceeded by barrier-less formation of an insertion complex CH_3BeOH while ZnO + CH_4 needed overcome a 36.7 kcal/mol barrier.

3.1.2. Decomposition

As shown in Fig. 2, the ^{3}IM2 is the most stable on the whole potential energy surface, with bound energy of 9.1 kcal/mol. NBO analysis shows that the C–Be and Be–2H bonds of ^{3}IM2 are weak. Using relaxed PES scan by enlarging the distance of Be–C or Be–2H by 0.1 Å each step, it has been confirmed that ^{3}IM2 can directly decompose to HBe + CH_3 or $BeCH_3$ + H. These two reaction pathways are exothermic by 7.8 kcal/mol and 6.7 kcal/mol, respectively, and the products BeH and $BeCH_3$ are both observed in the experiment [12]. The calculated bond length for BeH is 1.345 Å, which is in good agreement with experiment (1.345 Å) and ab initio calculation by RCCSD(T)/aug-cc-pVQZ [27,28]. The calculated $BeCH_3$ has C_{3v} geometry and the C–Be bond length is 1.681 Å.

3.1.3. Isomerization

In addition to direct decomposition, the ^{3}IM2 can isomerize to ^{3}IM3 through α-H migration from C to Be via transition state ^{3}TS2, which lies 17.1 kcal/mol above ^{3}IM2 and 8.0 kcal/mol above the initial reactants of Be(^{3}P) + CH_4. For ^{3}IM3, the energy is almost equal to initial reactants, and the optimized structure is planar with two different Be–H bond lengths and two different H–Be–C bond angles. IRC calculation for ^{3}TS2 reveals that CH_3 moiety of ^{3}IM2 firstly rotates about 60° to make 3H atom lying on the another side of C–Be bond and then 3H gradually leave C atom to form ^{3}IM3, $(H)_2$–Be–CH_2. It is noted that the C–Be bond in ^{3}IM3 has a feature of double-bond but its distance (1.730 Å) is longer than the single-bond value of 1.681 Å in $BeCH_3$, indicating the weak interaction between C and Be atoms. To reinforce the interaction between C and Be, the ^{3}IM3 further isomerizes to another more stable intermediate ^{3}IM4 via ^{3}TS3 with a very small barrier of 0.3 kcal/mol, as shown in Fig. 2. As a result, the C–Be bond of ^{3}IM4 is shortened to 1.649 Å. Although the calculated ^{3}IM4 is of planar C_{2v} symmetry with two equal Be–H bonds of 1.429 Å, there is no possibility to form one Be–C bond and two Be–H bonds since Be is electron-deficient atom (only two valance electrons). Therefore, 3H atom may leave Be atom to form H + $HBeCH_2$ channel, which can be examined by a relaxed PES scan. This channel is exothermic by 2.2 kcal/mol and can be observed experimentally in reference [12]. The calculated $HBeCH_2$ has planar C_{2v} structure and the Be–H and C–Be bonds are 1.328 Å and 1.646 Å, respectively.

From ^{3}IM4, the reaction can further proceed via four-center transition state ^{3}TS4 to form H_2 + HBeCH channel, which is exothermic by 11.1 kcal/mol. In ^{3}TS4, 3H and 5H atoms become closer to each other, with a distance of 1.202 Å, and meanwhile, the distances of Be–3H and C–5H become longer. The calculated energy barrier of this step is 25.5 kcal/mol relative to ^{3}IM4 and 19.2 kcal/mol relative to the reactants. IRC analysis shows that there is no two-molecule complex of H_2 and HBeCH in the exit potential energy surface, and the free H_2 and HBeCH will be formed directly through this transition state. The calculated product HBeCH is linear ($^3\Sigma$) with Be–H bond of 1.326 Å and C–Be bond of 1.610 Å. According to previous ab initio calculation [29], HBeCH($^3\Sigma$) has a ground-state isomer, $BeCH_2$, which has C_{2v} symmetry ($^3B_1$) and lies 2.9 kcal/mol lower in energy than HBeCH($^3\Sigma$). However, the calculations also show that the barrier between these two isomers is 50.0 kcal/mol and suggest that they can exist independently. We also try to find the reaction pathway of $BeCH_2$ + H_2 but fail. This is consistent with the experimental observation since no feature of $BeCH_2$ has been identified in the experiment.

As discussed above, for the reaction Be(^{3}P) + CH_4, the four possible reaction pathways can be formed through the insertion intermediate ^{3}IM2 followed by direct dissociation or further isomerization, and all channels are exothermic. As shown in Fig. 2, the most favorable channels are BeH + CH_3 and H + $BeCH_3$ and the least favorable one is H_2 + HBeCH because it must surmount a relatively high barrier ^{3}TS4. Therefore, the competition of H_2 + HBeCH with other channels is inefficient. However, the relatively intense spectrum of product HBeCH was experimentally observed in the reaction of laser-ablated Be atom with CH_4 [12]. This may be ascribed to the action of the photolysis in matrix experiment. The experimental results indicated that following the photolysis, the spectral intensities of products BeH and $BeCH_3$ decreased while those of $HBeCH_2$ and HBeCH increased and the increase of HBeCH was more remarkable. These results are consistent with our theoretical calculations since the four reaction channels are competitive to each other.

3.2. Singlet potential energy surface

The singlet–triplet splitting energy between Be(^{1}S) and Be(^{3}P) was calculated as 56.7 kcal/mol and 63.5 kcal/mol at UB3LYP/6-311G(d) and QCISD(T)/6-311++G(d,p) levels, respectively, which were in good agreement with the experimental value of 62.8 kcal/mol [30].

As shown in Fig. 3, the reaction of CH_4 with Be(^{1}S) leads to the formation of the $HBeCH_3$(^{1}IM1) in the $^1A_1$ ground-state with C_{3v} geometry, via the three-center transition state ^{1}TS1. This transition state has Cs symmetry and two C–H bonds are activated meanwhile, one elongating to 1.164 Å and the other elongating to 1.567 Å. The insertion angle C–Be–2H of ^{1}TS1 is 59.0° and larger than that in ^{3}TS1 (40.4°). However, the energy barrier for this step is predicted to be 60.5 kcal/mol above the ground reactants. Therefore, the ground-state Be(^{1}S) difficultly reacts with methane and the product $HBeCH_3$($^1A_1$) observed in the experiment [12] should result from an intersystem crossing between the triplet and singlet potential energy surfaces. We locate the crossing points (CP) by means of the intrinsic reaction coordinate (IRC) approach used by Yoshizawa et al. [31], namely, starting from ^{3}IM1 to ^{3}IM2 via ^{3}TS1, each optimized point along the IRC path was submitted to a single-point

energy calculation with the singlet electronic state. As a result, two crossing points have been located and both occur after passing the transition state ^{3}TS1, as shown in Fig. 4. It can be seen that the role of the first CP1 can be ignored since it lies in the left of the ^{1}TS1 and need overcome a 12.0 kcal/mol barrier to arrive at ^{1}IM1. The second CP2, which lies in the vicinity of ^{3}IM2, opens the possibility for an intersystem crossing to form the ground-state product $HBeCH_3(^1A_1)$. The insertion angle C–Be–2H in the second CP is about 76.0° and slightly smaller than that in ^{3}IM2 (78.0°). The $HBeCH_3(^1A_1)$ is the most stable on the whole PES, with 31.7 kcal/mol below the ground-state reactants $Be(^1S) + CH_4$ and 95.2 kcal/mol below the excited state reactants $Be(^3P) + CH_4$.

4. Conclusion

The potential energy profiles and mechanisms of the reaction between $Be(^3P, ^1S)$ and CH_4 have been investigated at QCISD(T)/6-311++G(d,p)//UB3LYP/6-311G(d) levels. The calculations show that the excited $Be(^3P)$ atom spontaneously inserts into C–H bond of methane to form the insertion intermediate $H–Be–CH_3(^3A')$, which can either directly decompose to BeH + CH_3 and H + $BeCH_3$ or isomerize and lead to the channels H + $HBeCH_2$ and H_2 + HBeCH. In addition, the $H–Be–CH_3(^3A')$ has access to the formation of ground-state $HBeCH_3(^1A_1)$ via an intersystem crossing between the triplet and singlet potential energy surfaces. Our calculations are well consistent with the experimental observations.

Acknowledgements

The present work was supported financially by the Natural Science Foundation of China (NSFC, No. 20903002) and Talent Group Construction Foundation of Anhui University (Grant No. 02203104/04).

Appendix A. Supplementary material

Supplementary material associated with this article can be found, in the online version, at doi:10.1016/j.theochem.2009.11.037.

References

[1] G.A. Ozin, D.F. McIntosh, S.A. Mitchell, J. Am. Chem. Soc. 103 (1981) 1574.
[2] J.M. Parnist, G.A. Ozin, J. Phys. Chem. 93 (1989) 1204.
[3] N.L. Sommaire, F. Legay, Chem. Phys. 211 (1996) 367.
[4] S. Castillo, A. Ramírez-Solís, E. Poulain, J. Quan. Chem. 27 (1993) 587.
[5] S. Castillo, A. Ramírez-Solís, D. Díaz, E. Poulain, Mol. Phys. 81 (1994) 825.
[6] P.E.M. Siegbahn, M. Svensson, R.H. Crabtree, J. Am. Chem. Soc. 117 (1995) 6758.
[7] M.E. Alikhani, Chem. Phys. Lett. 313 (1999) 608.
[8] H.M. Himmel, A.J. Downs, T.M. Greene, Chem. Rev. 102 (2002) 4191.
[9] L. Andrews, Organometallics 25 (2006) 4040.
[10] G.T. de Jong, D.P. Geerke, A. Diefenbach, F.M. Bickelhaupt, Chem. Phys. 313 (2005) 261.
[11] T.M. Greene, L. Andrews, A.J. Downs, J. Am. Chem. Soc. 117 (1995) 8180.
[12] T.M. Greene, D.V. Lanzisera, L. Andrews, A.J. Downs, J. Am. Chem. Soc. 120 (1998) 6097.
[13] H.J. Himmel, A.J. Downs, T.M. Greene, L. Andrews, Organometallics 19 (2000) 1060.
[14] H.G. Cho, L. Andrews, Organometallics 28 (2009) 1358.
[15] H.G. Cho, L. Andrews, Organometallics 26 (2007) 4098.
[16] M.R.A. Blomberg, P.E.M. Siegbahn, M. Svensson, J. Am. Chem. Soc. 114 (1992) 6095.
[17] Y. Shiota, K. Yoshizawa, J. Am. Chem. Soc. 122 (2000) 12317.
[18] A.D. Becke, J. Chem. Phys. 98 (1993) 1372.
[19] C. Lee, W. Yang, R.G. Parr, Phys. Rev. B 37 (1988) 785.
[20] M.J. Frish, et al. GAUSSIAN 03 (Reversion B.01) Gaussian, Inc., Pittsburgh, PA, 2003.
[21] J.H. Wang, H. Umemoto, A.W.K. Leung, W.H. Breckenridge, J. Chem. Phys. 104 (1996) 9401.
[22] N.L. Sommaire, F. Legay, J. Phys. Chem. A 102 (1998) 8759.
[23] H. Luna-García, S. Castillo, A. Ramírez-Solís, J. Chem. Phys. 110 (1999) 11315.
[24] H. Luna-García, S. Castillo, A. Ramírez-solís, J. Chem. Phys. 107 (1997) 6627.
[25] D.Y. Hwang, A.M. Mebel, Chem. Phys. Lett. 348 (2001) 303.
[26] Z.S. Su, S. Qin, D.Y. Tang, H.Q. Yang, C.W. Hu, J. Mol. Structure: THEOCHEM 778 (2006) 41.
[27] F.B.C. Machado, O. Roberto-Neto, F.R. Ornellas, Chem. Phys. Lett. 284 (1998) 293.
[28] M.Y. Gong, Z.Q. Wang, Y. Zhang, E.Y. Feng, Z.F. Cui, J. Mol. Structure: THEOCHEM 857 (2008) 44.
[29] B.T. Luke, J.A. Pople, P.R. Schleyer, Chem. Phys. Lett. 97 (1983) 265.
[30] http://physics.nist.gov/physRefdata.
[31] K. Yoshizawa, Y. Shiota, T. Yamabe, J. Chem. Phys. 111 (1999) 538.